Latin American Journal of Solids and Structures
www.lajss.org

Ballistic Limit of High-Strength Steel and Al7075-T6 Multi-Layered Plates Under 7.62-mm Armour Piercing Projectile Impact

Abstract

This paper presents the computational-based ballistic limit of laminated metal panels comprised of high strength steel and aluminium alloy Al7075-T6 plate at different thickness combinations to necessitate the weight reduction of existing armour steel plate. The numerical models of monolithic configuration, double-layered configuration and triple-layered configuration were developed using a commercial explicit finite element code and were impacted by 7.62 mm armour piercing projectile at velocity range of 900 to 950 m/s. The ballistic performance of each configuration plate in terms of ballistic limit velocity, penetration process and permanent deformation was quantified and considered. It was found that the monolithic panel of high-strength steel has the best ballistic performance among all panels, yet it has not caused any weight reduction in existing armour plate. As the weight reduction was increased from 20-30%, the double-layered configuration panels became less resistance to ballistic impact where only at 20% and 23.2% of weight reduction panel could stop the 950m/s projectile. The triple-layered configuration panels with similar areal density performed much better where all panels subjected to 20-30% weight reductions successfully stopped the 950 m/s projectile. Thus, triple-layered configurations are interesting option in designing a protective structure without sacrificing the performance in achieving weight reduction.

Keywords

Ballistic impact; ballistic limit; double-layered plate; numerical simulation; triple-layered plate

N. A. Rahman [a]
S. Abdullah [b *]
W. F. H. Zamri [c]
M. F. Abdullah [d]
M. Z. Omar [e]
Z. Sajuri [f]

Department of Mechanical and Materials Engineering, Faculty of Engineering and Built Environment, Universiti Kebangsaan Malaysia, 43600 UKM Bangi, Selangor, Malaysia.
[a] najihah.ar@gmail.com
[b] shahrum@ukm.edu.my
[c] fathul@eng.ukm.my
[d] m.faizal@upnm.edu.my
[e] zaidiomar@ukm.edu.my
[f] zsajuri@ukm.edu.my

*Corresponding author:
shahrum@ukm.edu.my

http://dx.doi.org/10.1590/1679-78252657

Received 25.11.2015
In revised form 01.04.2016
Accepted 04.04.2016
Available online 12.04.2016

1 INTRODUCTION

The recent trend in military industry is to incorporate lightweight materials into the armoured vehicle designs to reduce the vehicle weight in order to improve the fuel consumption efficiency and vehicle maneuverability, without sacrificing the performance and safety. Main criteria for an armour vehicle performance is to be able to withstand the ballistic impacts. Ballistic impact is an impact from low mass, high velocity projectile caused by a propelling source. The ballistic limit velocity is an important parameter in studying of the high velocity impact. Ballistic limit velocity is the impact velocity that gives the impactor the ability for full penetration without any residual energy (Børvik et al., 2009). Steels have been widely utilized in armour applications for their high strength and cheaper production (Übeyli et al., 2007). However, steel has restricted the mobility of armoured vehicle since it has relatively high density. This characteristic has been a disadvantage of an armour steel which has directed the researchers to find lighter materials to be integrated with existing armour steel satisfying the same level of protection (Übeyli et al., 2011).

Aluminium and its alloys offers a considerable potential for reducing the weight of an armoured vehicle body due to their high stiffness-to-weight ratio, good formability, good corrosion resistance, and recycling potential (Manes et al., 2014). The interest for aluminium alloys is not new. Several investigations have been carried out to reveal the ballistic resistance of different aluminium alloys. It has been observed that aluminium has some weaknesses compared to high strength steel when dealing with structural impact. It has lower Young's modulus, strength and ductility. It melts at much lower temperature about 700 to 800 K, comparing to high strength steel which melts above 1800 K. Since aluminium plate have poor ballistic performance, they are often utilized in multi-layered or spaced structures, in combination of other materials. Layering aluminium plate with high strength steel has become an interest in reducing the overall density of armour vehicle body while improving the ballistic perforation resistance. It has been shown that a hard surface front layer (high strength steel) erodes the projectile into fragments and acts as disruptor to the armour system while the soft ductile inner layer (aluminium alloys) absorbs the kinetic energy through plastic deformation and prevents unwanted projectile fragments from penetrating and acts as the absorber to the armour system. Sometimes the system requires another layer acting as backing layer or cover layer in the structures.

The experimental approach can provide good perforation results, but it is very expensive. On the other hand, the computer simulation has been proven to be a powerful and economical tool for the prediction of penetrations and perforations of deformable projectiles over all ranges of striking velocities (Erice et al., 2014; Kiliç and Ekici, 2013). Therefore, recently many scholars concentrated on using the finite element method to study the behaviour of developed materials under ballistic impacts. They integrated different kinds of aluminium alloys with existing armoured steel to reduce the weight. It has been demonstrated that the use of aluminium and its alloys offers a considerable potential for reducing the weight of an armoured vehicle body. Forrestal et al. (2010) studied the performance of laminated armour steel and aluminium alloys structure under ballistic impacts and found that Al7075-T6 and Al5083-H116 can be integrated with armour steel to serve as vehicle protective structures. Flores-Johnson et al. (2011) modelled the impact of a 7.62 mm APM2 projectile on multi-layered armour plates to investigate the effect of different layer configurations, thicknesses and material properties on ballistic performance. They found a good agreement between ballistic limit velocity from simulation and experimental data. Ubeyli et al. (2014) investigated the effect of laminate configuration

on the behaviour of aluminium laminated composite against 7.62 AP projectiles and found that using hard material on the first layer and aluminium alloy on the back layer can improve the ballistic performance of an armour steel. An investigation conducted by Dey et al. (2004) on the ballistic resistance of Weldox 700E steel against 7.62 mm APM2 projectiles at velocity of 850 m/s shows that 12 mm monolithic layer has slightly better ballistic performance than double-layered plates with same thickness. Later on, Teng et al. (2007) found out that ballistic resistance of a multi-layered panel depends on several factors such as projectile nose shape and impact velocity, layer configuration and material properties for both projectile and plates.

The studies mentioned earlier have shown that the penetration effects of multi-layered plates are complex problem and for design purposes, the factors such as layer configurations and thickness should be well considered to obtain optimum protective structures. Since different thickness of layers would give different ballistic performance, the study for different layering configuration has become necessary. Therefore, the aim of this study is to analyse the effect of different layer configurations (monolithic, double-layered and triple-layered), total weights and initial velocities to the ballistic limit velocity, penetration process and permanent deformation under a ballistic testing against 7.62 mm APM2 projectile. A series of finite element analysis for different thicknesses of high strength steel and aluminium panels at a range of impact velocities of 900 to 950 m/s were conducted to analyse the effects.

2 METHODOLOGY

2.1 Computational Modelling

The commercial explicit finite element code ASNSYS-AUTODYN version 13 was used for all finite element modeling of projectile and target plates. A 7.62 mm APM2 projectile was used at initial velocities ranging from 700 m/s to 1200 m/s. Initial velocity was chosen according to NATO STANAG 4569 ballistic protection level 3 which is 930 $\pm$20 m/s (NATO STANAG, 2004). However, decreasing and increasing the initial velocity was necessary to obtain the ballistic limit of the targets. Two material were used to design the double-layered and triple-layered target plates: HSS and Al7075-T6. The target plate was modelled as 50 mm diameter circular plate and fully clamped at the edge boundaries as in Figure 1(a). The projectile was modelled in three independent parts: Brass jacket, steel core and lead filler, and its geometries are shown in Figure 1(b). The target plate was modelled as 50 mm diameter circular plate and fully clamped at the edge boundaries.

In finite element analysis, the problem was considered as axisymmetric model taken into account that the bullet rotation does not come into consideration as in this study the main interest is the behaviour of impacted panel. A constant mesh size of 0.5 mm was selected to finely resolve each problem and make the through thickness elements for the penetration process to be 50 elements. The meshing elements of the target plate and projectile were constructed using mixed of quadrilateral and triangular elements. Contact condition used between plates and projectile is trajectory contact. Node-to-node connectivity was applied using pure langrage algorithm with implementation of geometric erosion where geometric erosion strain of two was chosen for HSS material to remove the elements experiencing large distortion and consequently, simulation failure can be avoided.

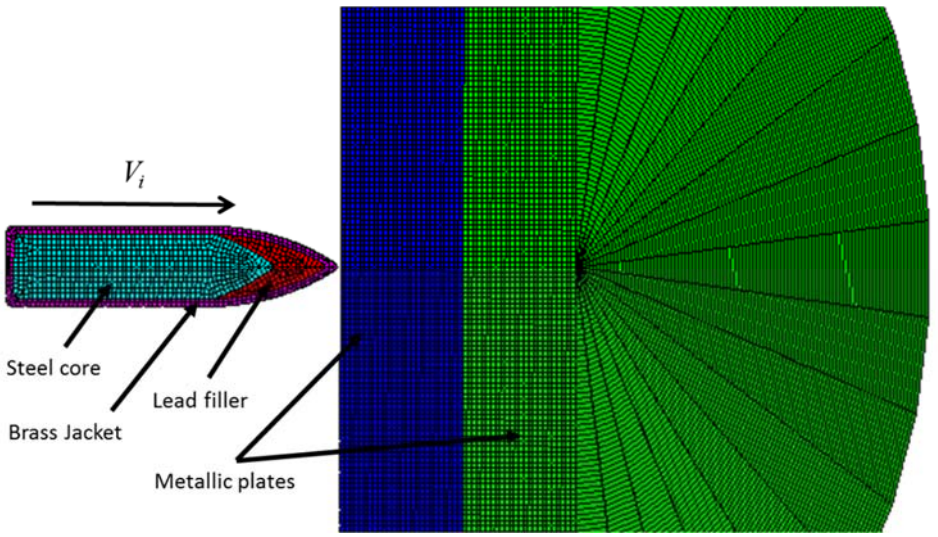

(a)

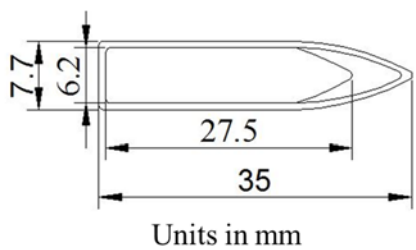

(b)

Figure 1: (a) FEA model of 7.62mm APM2 projectile and double-layered target, (b) Geometric of projectile.

The target configurations used in this study are summarized in Table 1. Three types of configurations were chosen: monolithic, double-layered and triple-layered. All panels have same total thickness of 25 mm. The important factor in the sample size is its thickness because the selected thickness of 25 mm is the standard thickness of existing armour panel (Zhou and Stronge, 2008). Each layer thickness was set accordingly to a range of 20% to 30% weight reduction of original armour panel to ensure the body maintaining on the ground during extreme conditions. The letters used as codes in Table 1 represent the layering configuration and type of material: M, monolithic, D, double-layered, T, triple-layered, H, high strength steel and A, Al7075-T6, whereas the numbers represent the thickness of the targets. For double-layered configurations, the target thickness for first layer made of HSS ranges from 13 mm to 17 mm and second layer made of Al7075-T6 ranges from 8 mm to 12 mm. Triple-layered configurations on the other hand consists of first and third layer thickness made of HSS ranging from 6mm to 9 mm, and second layer thickness made of Al7075-T6 ranging from 8 mm to 12 mm.

Configuration	Code	Areal density (kg/m2)	Mass reduction (%)	Initial impact velocity, V_i (m/s)
Monolithic	MH25	196.5	0	900-950
	MA25	70.1	64.3%	
Double-layered	DH17A08	156.1	20.6%	
	DH16A09	151	23.2%	
	DH15A10	145.9	25.7%	
	DH14A11	140.9	28.3%	
	DH13A12	135.8	30.9%	
Triple-layered	TH09A08H08	156.1	20.6%	
	TH08A09H08	151	23.2%	
	TH08A10H07	145.9	25.7%	
	TH07A11H07	140.9	28.3%	
	TH07A12H06	135.8	30.9%	

Table 1: Target plate configurations.

Both projectile and target panels used the Johnson-cook (JC) constitutive material model which has been commonly used for high velocity impact simulation (Kiliç and Ekici, 2013; Abdulhamid et al., 2013; Børvik et al., 2001). All projectile parts including hardened steel core, lead and brass jacket utilized the JC material constitutive model in order to avoid the stresses transmitted to the steel core were limited by the flow stress of the lead and brass jacket material because high velocity impact is affected by the temperature. The JC model is applied to determine the strain rate and temperature dependence of viscous-plastic material models and is expressed as,

$$\sigma_{eq} = \left(A + B\varepsilon_{eq}^{n}\right)\left(1 + \dot{\varepsilon}_{eq}^{n}\right)^{C}\left(1 - T^{*m}\right) \tag{1}$$

where σ_{eq} is the equivalent stress, ε_{eq} is the equivalent plastic strain, A, B, n, C and m are the material constants and $\dot{\varepsilon}_{eq}^{*} = \dot{\varepsilon}_{eq}/\dot{\varepsilon}_0$ is the dimensionless strain rate where it is a ratio of the strain rate and a user-defined strain rate. T^{*m} is the homologous temperature and is given by $T^{*m} = (T - T_r)(T_m - T_r)$, where T_r and T_m represent the room temperature and the melting temperature, respectively. This JC material model has been successfully implemented to model impact on steel (Abbasi et al., 2015) and aluminium targets (Forrestal et al., 2010). The JC parameters used in this study are shown in Table 2.

Material Properties	HSS	Al7075-T6	Steel core	Lead cap	Brass jacket
Density, ρ (kg/m3)	7860	2804	7850	10600	8520
Young's Modulus E, (GPa)	7.69	70	210	1	115
Poisson's ratio, ν	0.33	0.3	0.33	0.42	0.31
Yield Strength, A (MPa)	1250	480	1200	24	206
Strain Hardening, B (MPa)	362	520	1200	24	206
Strain Hardening exponent, n	1	477	50000	300	505
Strain rate constant, c	0.0108	0.001	0	0.1	0.1
Thermal softening constant, m	1	1	1	1	1.68
Melting temperature, Tm (K)	1800	893	1811	760	1189

Table 2: Material Properties and Modified Johnson-Cook model parameters (Abbasi et al., 2015; Forrestal et al., 2010).

2.1 Validation of FEA Model

FEA models were validated against the experiment data of Weldox 700E and Al7075-T651 from the literature. Weldox 700E was chosen to be compared with the high strength steel (HSS) used in this study because of their almost similar material properties in terms of density, Young's modulus and Poisson's ratio. The solid lines represent the Recht-Ipson model used to predict the residual velocity, V_r (Recht and Ipson, 1963),

$$V_r = a\left(V_i^P - V_{bl}^P\right)^{1/P} \tag{2}$$

Where a and P are empirical constants which best fit the data and V_{bl} is the ballistic limit. The original Recht-Ipson model indicates that $a = m_p/(m_p - m_{pl})$ and P=2, where m_p and m_{pl} denote the mass of the projectile and plug, respectively, and is applicable only if the plastic deformation of the projectile is negligible. Observations of experimental data from the literatures show that the penetration process of 7.62 mm APM2 projectile does not involve any significant plugging. Therefore, a was set as 1 and P was fitted to the data trend line. The method of least squares was used to obtain the best fit for P and V_{bl}.

Experimental data of the ballistic impact of 1x12mm of Weldox 700E, and 1x20 mm Al7075-T651 plates are compared with simulation data as shown in Figure 2. The ballistic limits of HSS and Al7075-T6 were obtained numerically by fitting the Recht-Ipson model in Eq. (2) to the simulation results. The solid lines in Figure 2 show good agreements between simulation data and experimental data from the literature. The simulation data established overestimation of ballistic limit with percentage differences about 7% and 13% for HSS and Al7075-T6, respectively. This overestimation maybe caused by the limitation of the constitutive model criterion and meshes used in the simulation. Pedersen et al. reported that meshing quality does affect the model accuracy and fine meshes can produce more accurate result compared to intermediate meshes (Padersen et al., 2011). However, in this study, intermediate meshes were used to reduce the computational effort and the results obtained show quite small differences between experimental and simulation data.

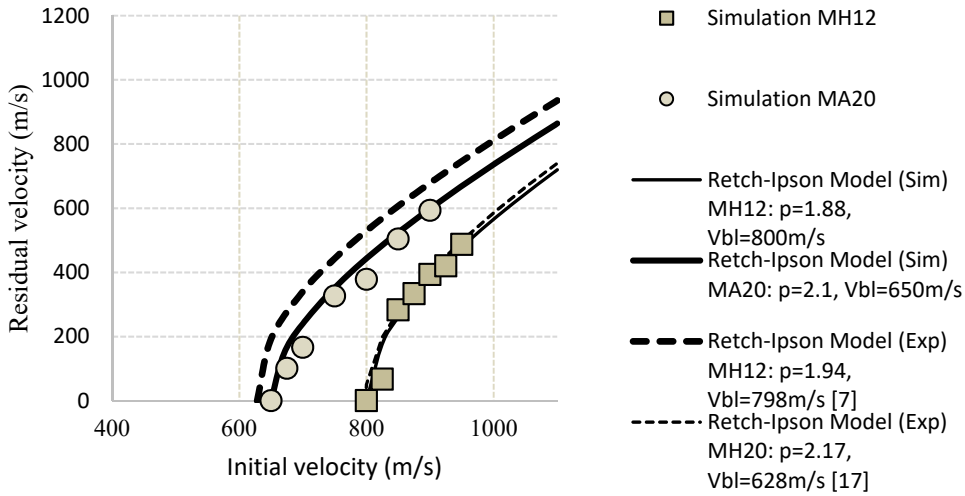

Figure 2: Comparison between experimental (Forrestal et al., 2010; Børvik et al., 2009) and predicted residual velocities.

Meshing analysis has been performed to determine the suitable mesh size for the finite element analysis. Mesh size was varied from 0.3mm to 1.0mm for the double-layered target plate and projectile as shown in Figure 3a-h. Depth of penetration for each model at initial velocity 900 m/s were evaluated as presented in Figure 4. The depth of penetration varies as the mesh size decreases from 1.0 mm to 0.6 mm. The variation becomes smaller as it is decreased from 0.5 mm to 0.3 mm. With taking into account the computational time, mesh size of 0.5 mm seems to be adequate for this finite element analysis.

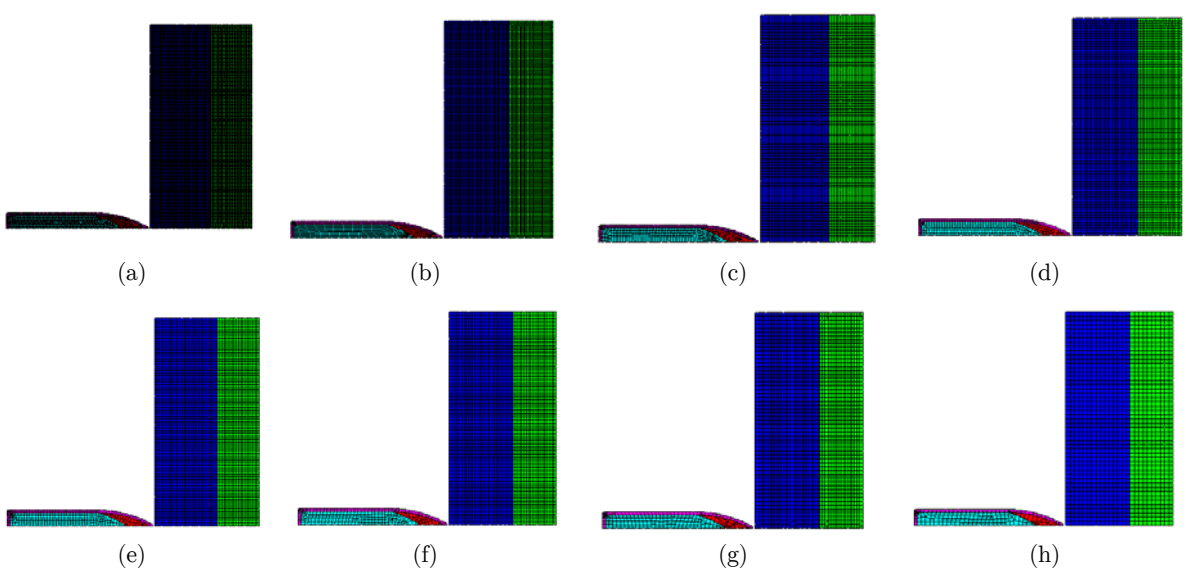

Figure 3: FE models for double-layered panels at mesh size of (a) 0.3 mm (b) 0.4 mm (c) 0.5 mm (d) 0.6 mm (e) 0.7 mm (f) 0.8 mm (g) 0.9 mm (h) 1.0 mm.

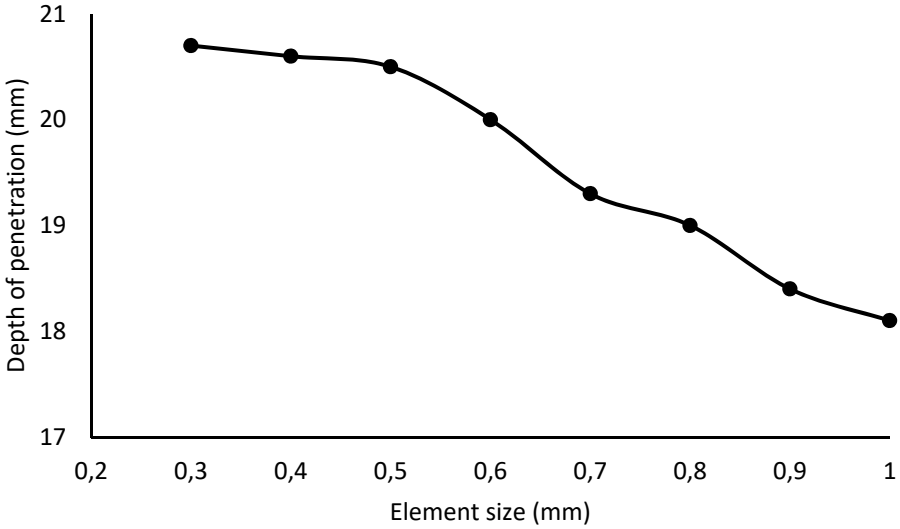

Figure 4: Depth of penetration of double-layered panels DH15A10 at projectile velocity of 900 m/s for mesh size 0.3 mm to 1.0 mm.

3 COMPUTATIONAL RESULTS AND DISCUSSIONS

3.1 Effect of multi-layered on ballistic limits

The effect of multi-layered laminated panels on the ballistic performance were studied using double-layered and triple-layered configuration panels of HSS and Al7075-T6 plates. Monolithic configuration panels of HSS and Al7075-T6 at thickness of 25 mm were also investigated to find the ballistic resistance limitation for multi-layered made of by mixing these two materials. Panels used in this study are tabulated in Table 1. The monolithic panels of MH25 and MA25 consist of 25 mm HSS plate and 25 mm Al7075-T6 respectively. Five double-layered panels of DH17A08, DH16A09, DH15A10, DH14A11 and DH13A12 consist of 17 mm, 16 mm, 15 mm, 14 mm and 13 mm thick HSS plate as front layer, and 8 mm, 9 mm, 10 mm, 11 mm and 12 mm thick Al7075-T6 plate as back layer, respectively. Other five triple-layered panels of TH09A08A08, TH08A09H08, TH08A10H07, TH07A11H07 and TH07A12H06 consist of 9 mm, 8 mm, 8mm, 7 mm and 7 mm thick HSS plate as front layer, 8 mm, 9 mm, 10 mm, 11 mm and 12 mm thick Al7075-T6 plate as intermediate layer, and 8 mm, 8 mm, 7 mm, 7 mm and 6 mm thick HSS plate as back layer, respectively.

The trend of ballistic performances for each target plate configuration set in Table 1 can be observed in Figure 5. The highest ballistic limit came from the monolithic plate of HSS which possesses the highest strength and areal density among all whereas the lowest ballistic limit came from the monolithic plate of Al7075-T6 which has the lowest strength and areal density. All ballistic limits of double-layered and triple-layered configuration panels laid between the ballistic limit of HSS and Al7075-T6. The ballistic limit of double-layered configuration panels varied for thickness differences. As the weight of 25 mm panel were reduced, the areal density of panel also reduced. This resulted in decreasing of ballistic limit from 980 m/s to 900 m/s as the weight was reduced from 20.6 % to 30.9 %. This reduction is explained by the fact that there is reduction in energy absorption capability of this

double-layered panels as the areal densities were reduced (Hou et al., 2010; Bürger et al., 2012). The same effect can be noticed from the triple-layered configuration panels. The same trend of decreasing in ballistic limits happened where they decreased from 1050 m/s to 975 m/s as the weight was reduced from 20.6% to 30.9%.

The ballistic limit for all panels were tabulated in Table 3 and Table 4. Statistically, the ballistic limit of Recht-Ipson model obtained were very convincing with R-square value of 0.92 to 0.99. The result indicates that all triple-layered panels attained higher ballistic limit compared to the double-layered panels of same areal density. The areal density affects the ballistic limit of target panel in terms of the ability of the target panel to absorb energy during impact. Panels with similar total thickness may differ in ballistic limit because of the ability of every layer constituting the multi-layered panel may differ. This indication raises an interesting issue on how the triple-layered panels exhibit greater ballistic resistance than the double-layered configuration possessing the same areal density. The issue is addressed in the next section by investigating the penetration process of both configuration panels.

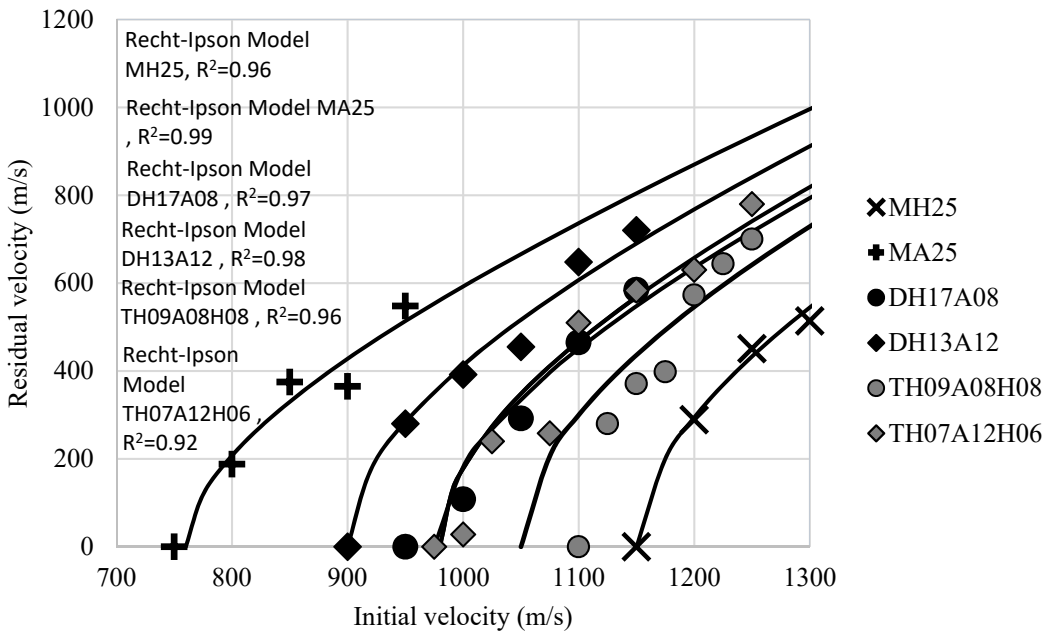

Figure 5: Residual velocity versus initial velocity for monolithic, double-layered and triple-layered configurations panels.

	MH25	MA25	DH17A08	DH16A09	DH15A10	DH14A11	DH13A12
a	1	1	1	1	1	1	1
Vbl	1150	760	980	960	940	920	900
P	1.8	1.84	1.9	1.9	1.84	1.82	1.92

Table 3: Ballistic limit and Recht-Ipson parameters for monolithic and double-layered target configuration panels.

	TH09A08H08	TH08A09H08	TH08A10H07	TH07A11H07	TH07A12H06
a	1	1	1	1	1
Vbl	1050	1020	1020	975	975
P	2.20	2.10	1.92	1.88	1.86

Table 4: Ballistic limit and Recht-Ipson parameters for triple-layered target configuration panels.

3.2 Effect of multi-layered on penetration process

Ballistic limit result has shown that triple-layered configuration has better performance than the double-layered configuration. Figure 6(a-d) show the penetrations of monolithic of MA25 and MH25 at time of 0.07 ms. At standard initial velocity of projectile 7.62 mm APM2 of 900 m/s and 950 m/s, projectile fully penetrated MA25 with residual velocity of 365 m/s and 548 m/s respectively which can be observed in Figure 6(a) and 6(b). Meanwhile the same velocity projectile was stopped by MH25 with residual thickness of 9 mm and 7 mm respectively as illustrated in Figure 6(c) and 6(d). Combination of these two materials using double-layered and triple-layered configurations produced variation of penetration as shown in Figure 7 and Figure 8. From Figure 7(a-j), it is observed that all double-layered panels had allowed 950 m/s projectile fully penetrated and had successfully stopped 900 m/s projectile. Among all, DH17A08 and DH16A09 as in Figure 7(a) and Figure 7(c) which possess areal density of 156 kg/m^2 and 151 kg/m^2 performed well at 900 m/s projectile with residual thickness of 4 mm and 2 mm respectively. This is undeniable because both have larger areal density compared to others and 151 kg/m^2 can be the limit areal density required for double-layered to successfully resist the 7.62 mm APM2 projectile.

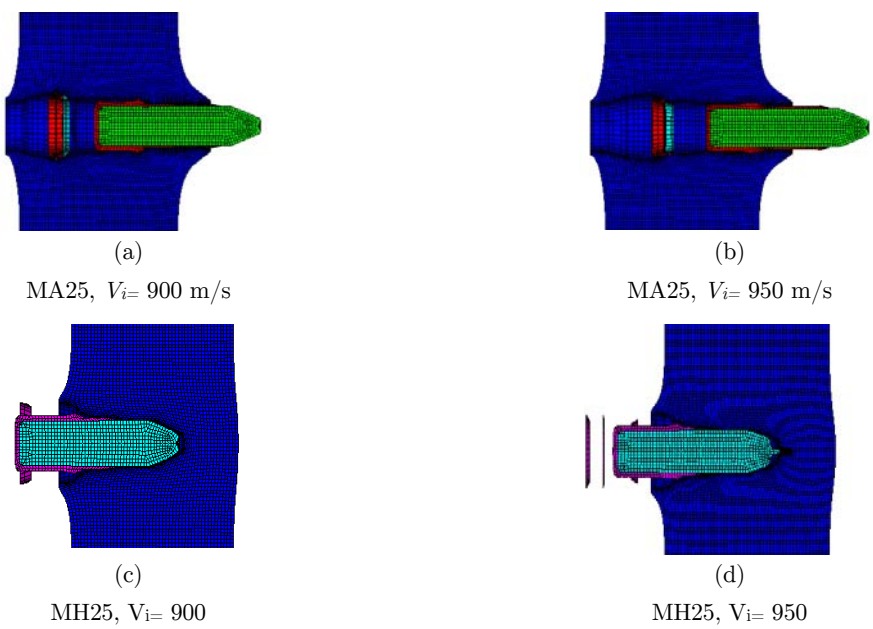

Figure 6: Penetration of projectile on monolithic configurations at 0.07 ms and initial velocity of 900 m/s and 950 m/s.

On the other hand, triple-layered panels as in Figure 8(a-j) have shown better projectile resistance compared to the double-layered panels. For both 900 m/s and 950 m/s projectiles, all triple-layered panels had successfully stopped the projectiles and these phenomena are proved by the ballistic limit resulting from Recht-Ipson model in Table 4. Again, panels with areal density of 156 kg/m^2 and 151 kg/m^2 as illustrated in Figure 8a and 8c resisted the 900 m/s projectile well with 4 mm and 3 mm residual thickness respectively. At this state, these two triple-layered panels seem to have similar performance with the double-layered. Nevertheless, the limit of areal density for triple-layered panels to resist the 7.62 mm APM2 projectile has increased up to 136 kg/m^2 which can allow greater weight reduction up to 30.6% compared to the double-layered panels for 23.2% only.

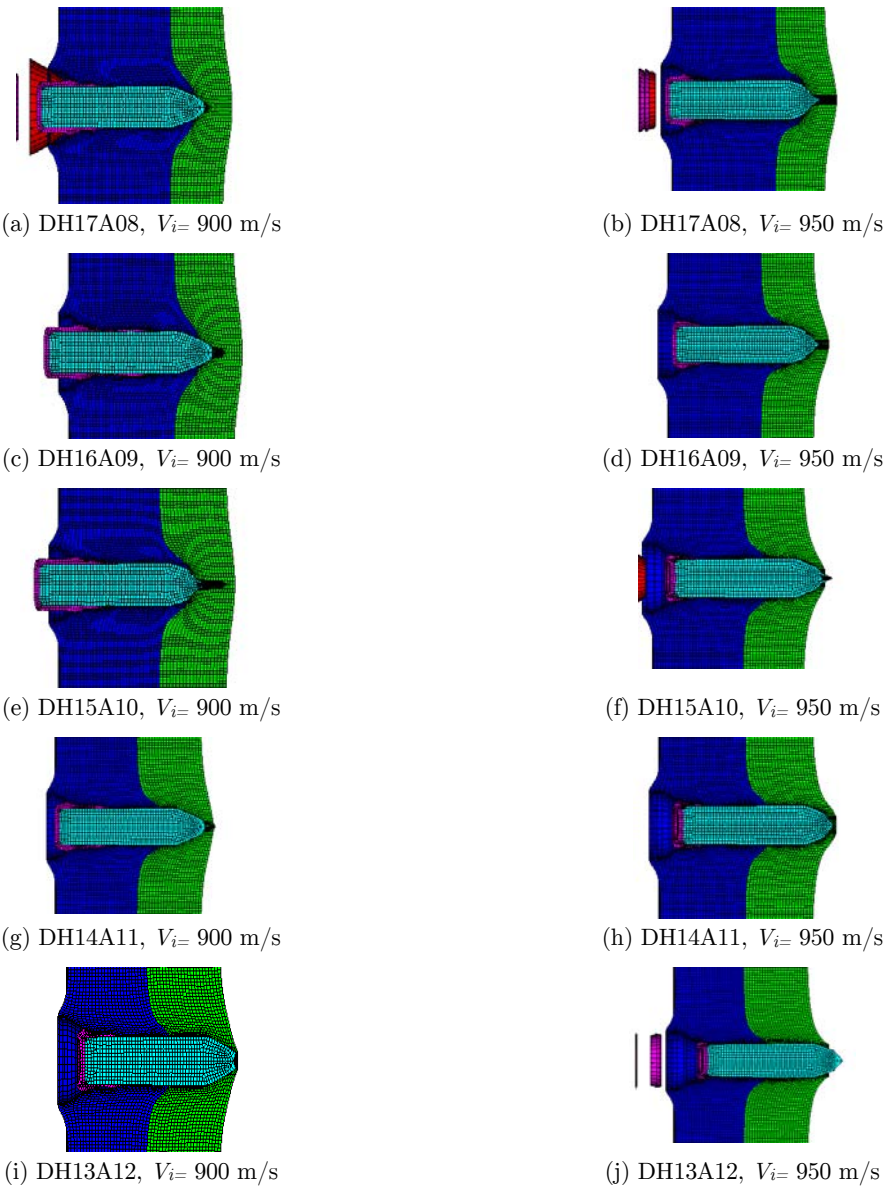

(a) DH17A08, V_i= 900 m/s (b) DH17A08, V_i= 950 m/s

(c) DH16A09, V_i= 900 m/s (d) DH16A09, V_i= 950 m/s

(e) DH15A10, V_i= 900 m/s (f) DH15A10, V_i= 950 m/s

(g) DH14A11, V_i= 900 m/s (h) DH14A11, V_i= 950 m/s

(i) DH13A12, V_i= 900 m/s (j) DH13A12, V_i= 950 m/s

Figure 7: Penetration of projectile on double-layered configurations at 0.07ms and initial velocity 900 m/s and 950 m/s.

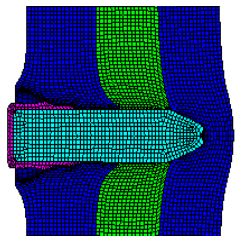

(a) TH09A08H08, $V_{i=}$ 900 m/s

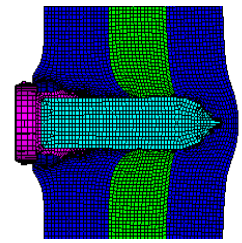

(b) TH09A08H08, $V_{i=}$ 950 m/s

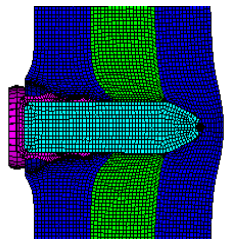

(c) TH08A09H08, $V_{i=}$ 900 m/s

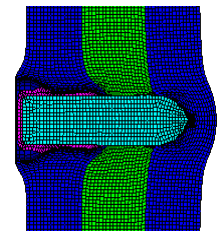

(d) TH08A09H08, $V_{i=}$ 950 m/s

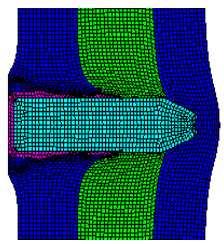

(e) TH08A10H07, $V_{i=}$ 900 m/s

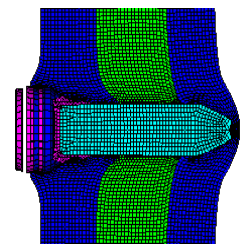

(f) TH08A10H07, $V_{i=}$ 950 m/s

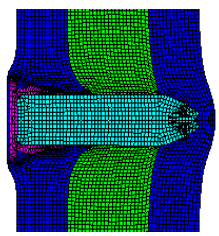

(g) TH07A11H07, $V_{i=}$ 900 m/s

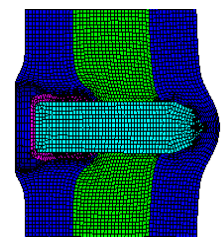

(h) TH07A11H07, $V_{i=}$ 950 m/s

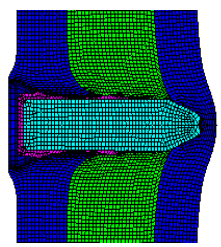

(i) TH07A12H06, $V_{i=}$ 900 m/s

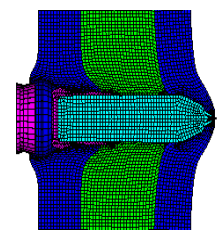

(j) TH07A12H06, $V_{i=}$ 950 m/s

Figure 8: Penetration of projectile on triple-layered configurations at 0.07ms and initial velocity 900 m/s and 950 m/s.

Figure 9(a) and 9(b) show the projectile velocity versus time for DH17A08 which represents panel with 20.6% weight reduction and DH13A12 which represents panel with 30.9% weight reduction, respectively, when impacted with an initial velocity of 950 m/s, the highest velocity of 7.62 mm

APM2 projectile could have. It can be seen that the penetration processes of these panels are quite similar. As the projectile entering the thick target plate, the core penetrated into the target while the brass jacket collapsed around the core indenting the target. The target plate experienced ductile-hole formation by the steel core and the brass jacket bounced backwards without penetration leaving a crater ring around the hole. The brass jacket was energetic enough to shear off a plug around the hole and moved for some distance for time 0.03 to 0.08 ms before breaking off at 0.08 ms. Similar behaviour during penetration process can be seen in Me-bar et al. (1997). DH17A08 stopped the projectile at 0.08 ms while DH13A12 was fully perforated at 0.08 ms with residual velocity of 280 m/s. Figure 10(a) and 10(b) display the projectile velocity versus time for TH09A08H08 which has same areal density with DH17A08 and TH07A12H06 which has same areal density with DH13A12, respectively, after being impacted by 950 m/s 7.62 mm APM2 projectile. Both had successfully stopped the projectile but at different time of 0.06 ms and 0.08 ms for TH09A08H08 and TH07A12H06 respectively. The gap of performance when the weight reduced from 20.6% to 30.9% is not varied too much in triple-layered panels compared to double-layered panels. This phenomenon will be discussed further in terms of permanent deformation caused by different layering configurations in next section.

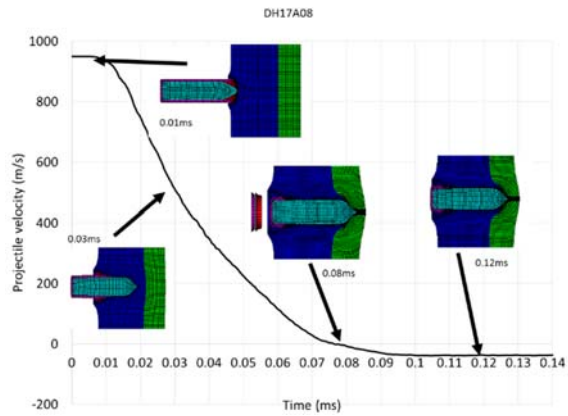

(a)

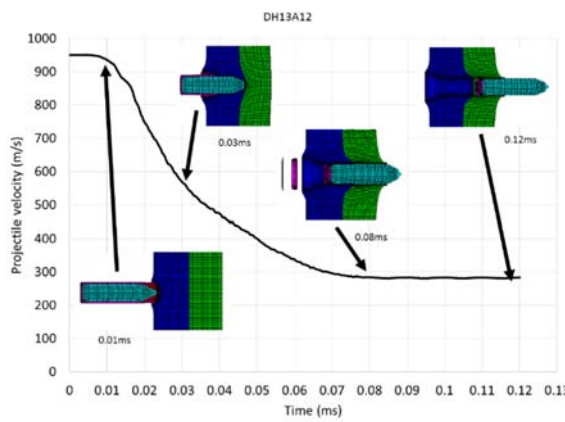

(b)

Figure 9: Penetration process of double layered configurations (a) DH17A08 (20.6% mass reduction), (b) DH13A12 (30.9% mass reduction), for an initial projectile velocity of 950 m/s.

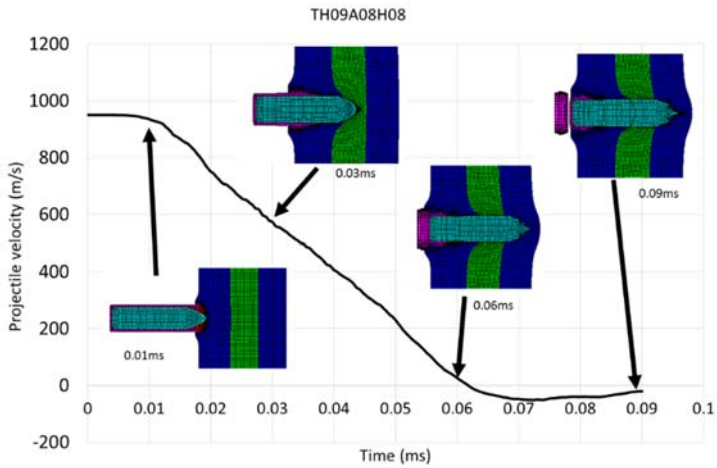

(a)

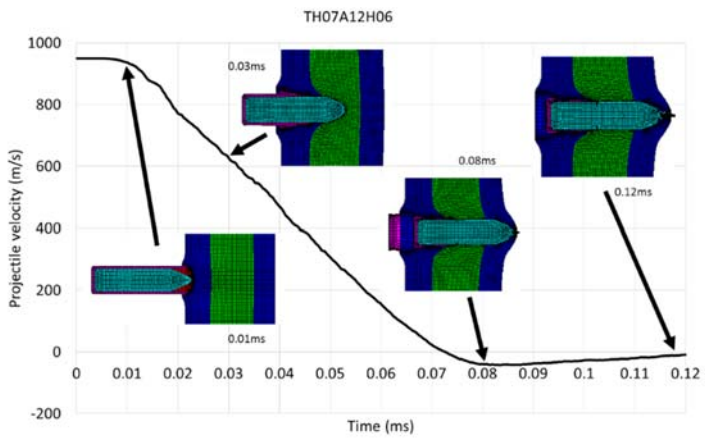

(b)

Figure 10: Penetration process of three-layered configurations (a) TH09A08H08 (20.6% mass reduction), (b) TH07A12H06 (30.9% mass reduction), for an initial projectile velocity of 900 m/s.

3.3 Effect of multi-layered on permanent deformation

Based on the ballistic limit and penetration process of the multi-layered panels, it is noticeable that the triple-layered configuration panels exhibits better performance than double-layered configuration panels of same areal density. This performance can be explained by the fact that triple-layered configuration has a backing plate made of HSS. It is believed that the third layer acts as backing plate support the second layer to increase its energy absorption capability (Ramadhan et al., 2013; Sudhir Sastry et al., 2014). Hence, the ability of first and second layer absorbed most of the kinetic energy from the projectile increased and stopped the projectile from penetrating the laminated panel. This behaviour can be observed in Figure 11-13 where the permanent deformation profiles for all configuration targets after being impacted by 950 m/s projectile are illustrated. Figure 11(a) shows the permanent deformation occurred on 25 mm monolithic HSS panel where the panel deformed about 1mm thick to stop the projectile at 20 mm depth of penetration. On the other hand, Figure 11(b)

shows the permanent deformation happened on 25 mm monolithic Al7075-T6 where the projectile fully perforated and caused the panel deformed about 5 mm thick. This phenomenon is supported by the fact that Al7075-T6 has more ductile and softer than the HSS (Forrestal et al., 2010; Mishra et al., 2012).

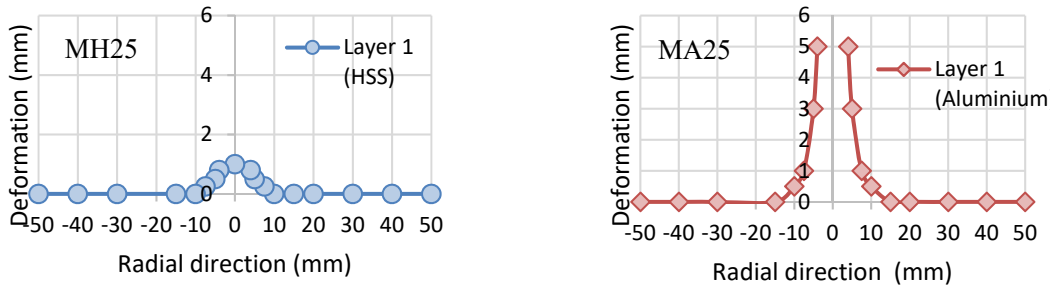

(a) (b)

Figure 11: Permanent deformation of monolithic configuration panels at initial velocity of 950m/s.

Mixing HSS and Al7075-T6 in layering form caused the permanent deformation to vary from one to another configuration. Figure 12(a) and 12(b) show that DH17A08 panel and DH16A09 are the best configuration among double-layered configuration panels which successfully stopped the 950 m/s projectile with 2mm and 3mm backing layer deformations respectively, while the rest of double-layered configuration panels as shown in Figure 10a-e failed to resist the 950 m/s projectile. For all double-layered cases, the first layer made of HSS deformed larger than second layer of Al7075-T6 because it absorbed the energy more than the second layer. As the areal density of double-layered panels was decreased, the second layer has to absorbed energy more and had caused it to deform larger. Quite similar phenomena can be seen from permanent deformation of the triple-layered when the areal density was reduced but different in the way of every layer deformed.

Figure 13 shows the permanent deformation of triple-layered configuration panels at 950 m/s projectile velocity. TH09A08H08 and TH08A09H08 as shown in Figure 13(a) and 12(b) are the best combination panels among all triple-layered configuration panels as they exhibit smaller layer deformations compared to others. For the rest of triple-layered configuration panels as shown in Figure 13(c-e), the first and second layers deformed at quite similar thick and radial direction because it is believed that they had fully absorbed the energy as they were capable to do. Whereas, the deformation of third layer increased as the areal density was reduced from Figure 13(a-e). The worst case for triple-layered happened at TH07A12H06 as seen in Figure 13(e) which possesses the lowest areal density and highest weight reduction. However, comparing to the same areal density and weight reduction of double-layered panel configuration DH13A12 as in Figure 12(e), it is better in term of ballistic performance. These findings show that an armour vehicle made of laminated panels of two different materials could potentially perform better than the existing armour steel plate with additional attribute of having lesser weight which would enhance maneuverability.

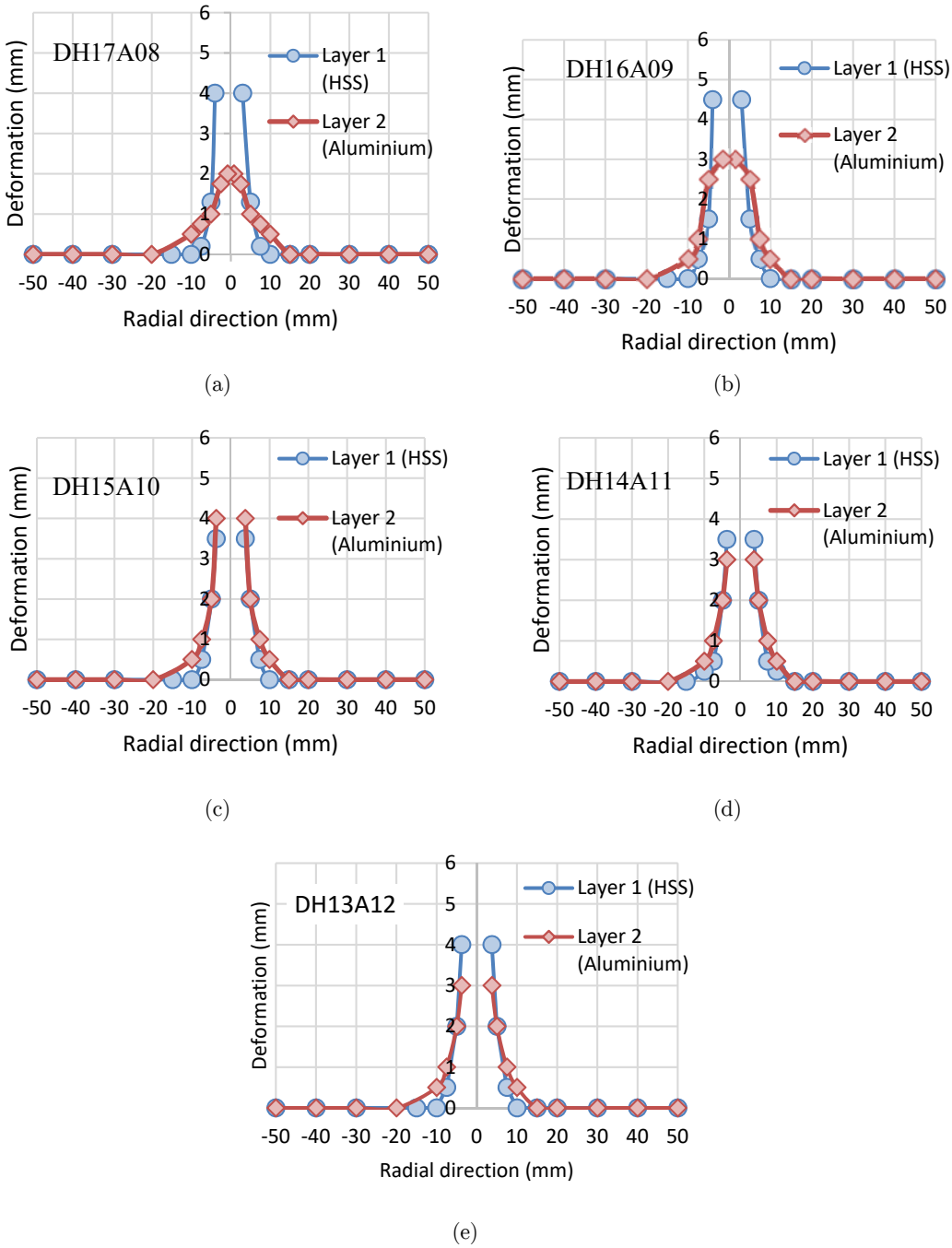

Figure 12: Permanent deformation of double-layered configuration panels at initial velocity of 950 m/s.

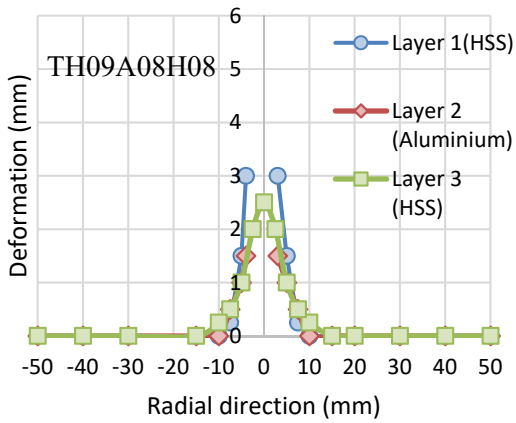

(a)

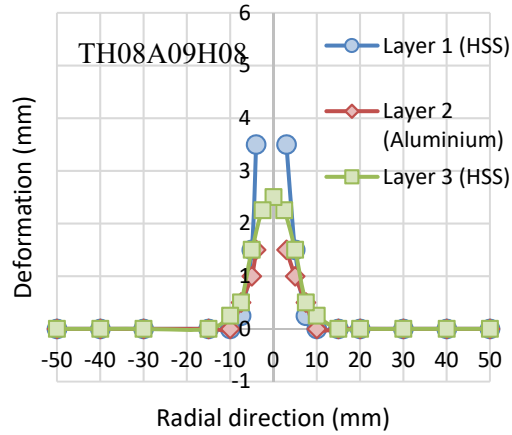

(b)

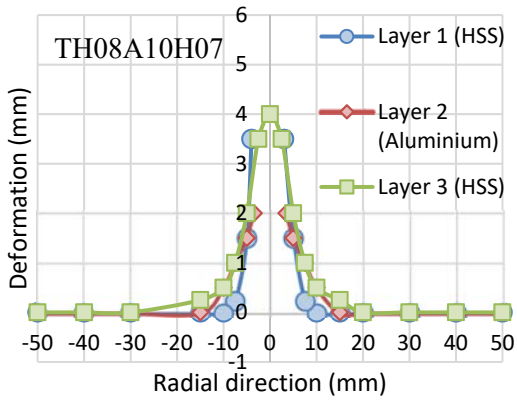

(c)

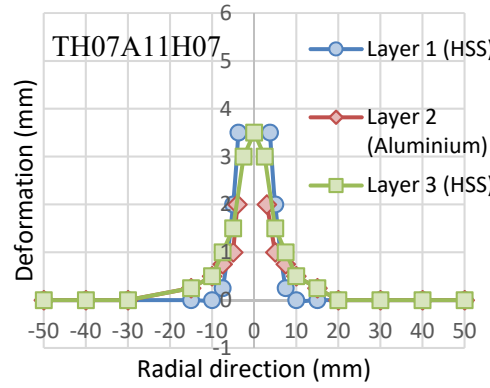

(d)

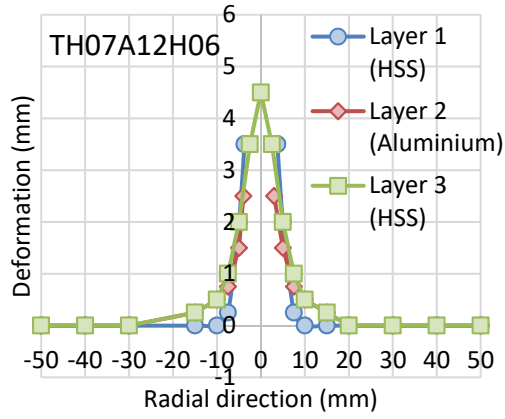

(e)

Figure 13: Permanent deformation of triple-layered configuration target panels at initial velocity of 950 m/s.

4 CONCLUSIONS

In summary, the computational simulation demonstrated the capability of the FEA model developed to predict the ballistic behaviour of HSS and Al7075-T6 laminated panels and could be used for the design of experimental testing which might lead to reduction of the number of necessary tests needed for this study later on. Nevertheless, this study is still computational based and experimental validation should be performed to prove the validity of the study. It was observed that the double-layered configuration panels became less resistance to ballistic impact as the weight reduction was increased from 20% to 30%, where only at 20% and 23.2% of weight reduction panel could successfully stopped the 950m/s projectile. However, with same areal density, the triple-layered configuration panels had performed 8% to 12% better than double-layered configuration. Panel TH08A09H08 with 23.2% weight reduction has the best performance among triple-layered panels with smallest depth of penetration of 21 mm. Thus, it is concluded that triple-layered configurations made with a combination of HSS and Al7075-T6 are interesting option for designing a protective structure as they potentially would lead to weight saving while improving the ballistic performance of the structure.

Acknowledgement

The authors wish to express their gratitude to Ministry of Higher Education Malaysia via Universiti Kebangsaan Malaysia and Universiti Pertahanan Nasional Malaysia under research funding LRGS/2013/UPNM-UKM/DS/04 for supporting this research project.

References

Abbasi, M., Reddy, S., Ghafari-Nazari, A., Fard, M. (2015). Multi-objective crashworthiness optimization of multi-cornered thin-walled sheet metal members. Thin-walled structures: 31-41

Abdulhamid, H., Kolopp, A., Bouvet, C., Rivallant, S. (2013). Experimental and numerical study of AA5086-H111 aluminum plates subjected to impact. International Journal of Impact Engineering 51:1-12.

Børvik, T., Dey, S., Clausen, A.H. (2009). Perforation resistance of five different high strength steel plates subjected to small-arms projectiles. International Journal of Impact Engineering 36:948-964.

Børvik, T., Forrestal, M.J., Hopperstad, O.S., Warren, T.L., Langseth, M. (2009). Perforation of AA5083-H116 aluminium plates with conical-nose steel projectiles - Calculations. International Journal of Impact Engineering 36(3):426-437.

Børvik, T., Langseth, M., Hopperstad, O.S., Malo, K. (2001). A perforation of 12mm thick steel plates by 20mm diameter projectiles with flat, hemispherical and conical noses - Part I: Experimental study. International Journal of Impact Engineerig 27(1):19-35.

Bürger, D., Rocha De Faria, A., De Almeida, S.F.M., De Melo, F.C.L., Donadon, M.V. (2012). Ballistic impact simulation of an armour-piercing projectile on hybrid ceramic/fiber reinforced composite armours. International Journal of Impact Engineering 43:63-77

Dey, S., Børvik, T., Hopperstad, O.S., Leinum, J.R., Langseth, M. (2004). The effect of target strength on the perforation of steel plates using three different projectile nose shapes. International Journal of Impact Engineering 30(8-9):1005-1038.

Erice, B., Pérez-Martín, M.J., Gálvez, F. (2014). An experimental and numerical study of ductile failure under quasi-static and impact loadings of Inconel 718 nickel-base superalloy. International Journal of Impact Engineering 69:11-24.

Flores-Johnson, E.A., Saleh, M., Edwards, L. (2011). Ballistic performance of multi-layered metallic plates impacted by a 7.62-mm APM2 projectile. International Journal of Impact Engineering 38(12):1022-1032.

Forrestal, M.J., Børvik, T., Warren, T.L. (2010). Perforation of 7075-T651 Aluminum Armor Plates with 7.62 mm APM2 Bullets. Experimental Mechanics 50(8):1245-1251.

Hou, W., Zhu, F., Lu, G., Fang, D.H. (2010). Ballistic impact experiments of metallic sandwich panels with aluminium foam core. International Journal of Impact Engineering 37:1045-1055.

Kiliç, N., Ekici, B. (2013). Ballistic resistance of high hardness armor steels against 7.62 mm armor piercing ammunition. Materials and Design 44:35-48.

Kiliç, N., Ekici, B. (2013). Ballistic resistance of high hardness armor steels against 7.62 mm armor piercing ammunition. Materials and Design 44:35-48.

Manes, A., Serpellini, F., Pagani, M., Saponara, M., Giglio, M. (2014). Perforation and penetration of aluminium target plates by armour piercing bullets. International Journal of Impact Engineering 69:39-54.

Me-bar, Y., Rosenberg, Z. (1997). On the correlation between the ballistic behaviour and dynamic properties of titanium-alloy plates. International Journal of Impact Engineering 19(4): 311-318.

Mishra, B., Jena, P.K., Ramakrishna, B., Madhu, V., Bhat, T.B., Gupta, NK. (2012). Effect of tempering temperature, plate thickness and presence of holes on ballistic impact behavior and ASB formation of a high strength steel. International Journal Impact Engineering 44:17-28.

NATO STANAG 4569. Protection levels for occupants of logistic and light armored vehicles, 1st ed.; 2004.

Padersen, K.O., Børvik, T., Hopperstad, O.S. (2011). Fracture mechanisms of aluminium alloy AA7075-T651 under various loading conditions, Material and Design 32:97-107.

Ramadhan, A.A., Abu Talib, A.R., Mohd Rafie, A.S., Zahari, R. (2013). High velocity impact response of Kevlar-29/epoxy and 6061-T6 aluminum laminated panels. Materials and Design 43:307-321.

Recht, R.F., Ipson, T.W. (1963). Ballistic perforation dynamics. Journal of Applied Mechanics 30:384-390.

Sudhir Sastry, Y.B., Budarapu, P.R., Krishna, Y., Devaraj, S. (2014). Studies on ballistic impact of the composite panels. Theoretical and Applied Fracture Mechanics 72:2-12.

Teng, X., Dey, S., Børvik, T., Wierzbicki, T. (2007). Protection performance of double-layered shields against projectile impact. Journal of Mechanics of Material Structures 2:1309-1329.

Übeyli, M., Balci, E., Sarikan, B., et al. (2014). The ballistic performance of SiC-AA7075 functionally graded composite produced by powder metallurgy. Material and Design 56:31-36.

Übeyli, M., Deniz, H., Demir, T., Ögel, B., Gürel, B., Keleş, Ö. (2011). Ballistic impact performance of an armor material consisting of alumina and dual phase steel layers. Material and Design 32(3):1565-1570.

Übeyli, M., Yildirim, R.O., Ögel, B. (2007). On the comparison of the ballistic performance of steel and laminated composite armors. Material and Design 28(4):1257-1262.

Zhou, D.W., Stronge, W.J. (2008). Ballistic limit for oblique impact of thin sandwich panels and spaced plates. International Journal of Impact Engineering 35(11):1339-1354.